

# Pressure densified 1,3,5-tri(1-naphthyl)benzene glass. I. Volume recovery and physical aging

Cite as: *J. Chem. Phys.* **151**, 184502 (2019); doi: [10.1063/1.5122765](https://doi.org/10.1063/1.5122765)

Submitted: 31 July 2019 • Accepted: 17 October 2019 •

Published Online: 11 November 2019



View Online



Export Citation



CrossMark

A. P. Holt,<sup>a)</sup>  D. Fragiadakis,<sup>b)</sup>  and C. M. Roland<sup>b)</sup> 

## AFFILIATIONS

Naval Research Laboratory, Chemistry Division, Washington, DC 20375-5342, USA

<sup>a)</sup>American Society for Engineering Education Postdoctoral Fellow.

<sup>b)</sup>[roland@nrl.navy.mil](mailto:roland@nrl.navy.mil)

## ABSTRACT

The effects of pressure densification on 1,3,5-tri(1-naphthyl)benzene (TNB) are assessed from volumetric and calorimetric measurements. The pressure densified glass (PDG) has higher density than conventional glass (CG), but unlike ultrastable TNB glass prepared using vapor deposition which also has elevated density, TNB PDG exhibits higher enthalpy and lower thermal stability than when formed at ambient pressure. PDG also exhibits anomalous physical aging. Rather than evolving monotonically toward the equilibrium density, there is an overshoot to a lower density state. Only when the density of the PDG becomes equivalent to the corresponding CG does the density begin a slow approach toward equilibrium.

Published under license by AIP Publishing. <https://doi.org/10.1063/1.5122765>

## INTRODUCTION

The utility of glasses makes them an obvious topic of research although their complex, nonequilibrium properties present challenges to investigations of structure-property relationships. There are various methods of forming a glass, some commercially important and others being developed; these fabrication techniques include tempering,<sup>1,2</sup> lamination,<sup>3,4</sup> bulk metallic alloying,<sup>5–7</sup> vapor deposition,<sup>8,9</sup> vitrification in a strong electric field,<sup>10,11</sup> anisotropic glasses,<sup>12</sup> and the use of pressure. This last method, known as pressure densification, is of interest herein. Pressure densification entails application of pressure prior to cooling of an equilibrium liquid to the glassy state. The resulting pressure densified glass (PDG) exhibits a higher density and different thermal and mechanical properties than the corresponding glass prepared by cooling at low pressure (conventional glass, CG).<sup>13–21</sup> Understanding, manipulating, and exploiting the full potential of PDG offer the possibility of better properties. We recently showed that pressure densified polymeric glasses become unstable at temperatures significantly lower than the glass transition temperature of the CG, which limits the utility of these materials at higher temperature and places an upper bound on the useful densification pressure.<sup>22</sup> However, glasses are in a nonequilibrium state which complicates fundamental studies, and the time-dependent behavior of PDG,

especially at temperatures close to the glass transition, is poorly understood.

Physical aging of a glass refers to the slow spontaneous decrease in volume and enthalpy accompanying evolution toward the liquid state. This lack of stability is a problem inherent to virtually all glasses as mechanical properties change, embrittlement being an obvious example. On the other hand, the equilibration pathway of a PDG is not obvious. For example, a PDG can be produced that has the density of the equilibrium liquid at that temperature and pressure.<sup>23–26</sup> However, since a glass inherits the structure of its liquid at the state at which it was formed,<sup>27,28</sup> the structure and configurational properties are close to those of the liquid at the substantially higher temperature and pressure at which the PDG was vitrified.

We carried out a study to characterize the stability, volume recovery, and physical aging of conventional and pressure densified glasses of TNB. TNB is a good glass-former, being readily quenched into an amorphous glass,<sup>29–33</sup> and as we show herein, it is highly responsive to pressure. TNB can also be vapor deposited to form a glass that exhibits higher density and unusual stability, corresponding to a conventional glass aged for centuries or longer.<sup>33,34</sup> Obtaining equilibrated glass is intriguing from a fundamental perspective, for example, in the search for a genuine phase transition that might underlie the glass transition.<sup>35,36</sup>

The practical consequences are obvious since physical aging becomes negligible, and thus, the properties become stable. However, PDG, despite being denser than CG, can have higher enthalpy and lower stability,<sup>25,26,37</sup> making the comparison of aging of these types of glasses especially interesting.

## EXPERIMENTAL

The glass former characterized herein was the ( $\alpha,\alpha,\alpha$ ) isomer of 1,3,5-tri(naphthyl)benzene (99% purity), purchased from TCI Chemicals and used as received.

Pressure-volume-temperature (PVT) measurements were performed with a Gnomix apparatus, which allows for *in situ* specific volume measurements over a wide range of temperatures (25–250 °C;  $\pm 0.25$  °C control) and pressures (10–200 MPa).<sup>38</sup> Prior to loading into the Gnomix device, the sample was degassed, heated above its melting point, then formed into a bubble-free, solid pellet. Pressure-densified samples were prepared by heating into the liquid state, applying pressure (>10 MPa), then cooling into the glass to 25 °C at the pressure, followed by the release of the pressure to 10 MPa (the minima for the instrument). To determine material properties other than specific volume, the pressure-densified glass was removed from the Gnomix apparatus at 25 °C, with subsequent measurements during heating. Therefore, there is a small time difference between the formation of the pressure-densified glass and measurement of thermodynamic properties (but transfer time between glass formation and the measurements was at least two orders of magnitude shorter than the recovery time).

Temperature-modulated differential scanning calorimetry (TM-DSC) was used (TA Q1000 with TA LNCS and calibrated using indium and sapphire) to determine the thermodynamic properties of conventional and pressure-densified glasses of TNB. For the measurement, the CG was equilibrated at 200 °C, followed by cooling to 20 °C at 0.5 °C/min. Both conventional and pressure-densified glasses were then measured upon heating at 0.5 °C/min to 200 °C with a modulation amplitude of 1 °C and a period of 60 s.

Dielectric spectra were obtained using a Novocontrol Alpha-A analyzer in conjunction with a Delta environment chamber. The samples were measured in a parallel plate geometry during both cooling and heating, with 2 °C increments over the range from 20 to 200 °C.

## RESULTS

### Vitrification of TNB

TNB was cooled to a glass at various pressures  $P_1$ , with representative results for a vitrification pressure of 200 MPa shown in Fig. 1. Releasing the pressure (to the minimum of our apparatus, 10 MPa, rather than ambient) reduces the density although it remains higher than  $\rho$  of the CG. This densification is an increasing function of  $P_1$ , as quantified by the parameter  $\delta$ ,<sup>39</sup>

$$\delta = \frac{v_{CG} - v_{PDG}(P_0)}{v_{CG} - v_{PDG}(P_1)}, \quad (1)$$

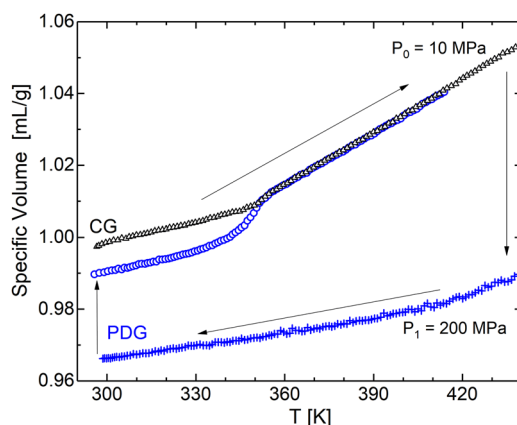


**FIG. 1.** Pressure densification of TNB at 200 MPa showing cooling under pressure (crosses), followed by heating after release of the pressure (circles). The heating curve is equivalent to that of the CG (triangles) beyond  $T_g$ , whereas the PDG is denser than the conventional glass.

in which  $P_0 = 10$  MPa herein and  $v_{CG}$  and  $v_{PDG}$  are the specific volumes of glass formed at  $P_0$  and  $P_1$ , respectively. In Fig. 2,  $\delta$  is plotted for vitrification pressures from 50 to 200 MPa. The values for TNB are at the upper end of the range of  $\delta$  reported for other PDGs.<sup>22,25,40–42</sup>

At the highest densification pressure herein ( $P_1 = 200$  MPa), the density of TNB increases almost 1% over  $\rho$  of the CG. In Fig. 2, the effect of densification pressure is seen to be leveling off, as seen previously for PDG,<sup>25</sup> with a similar effect also observed for their density fluctuations.<sup>43</sup> More substantial density increases are unlikely by a further increase in  $P_1$ , and in fact, a prior study of pressure densification of polycarbonate found that there is a maximum in  $\rho$  vs densification pressure, ascribed to the decreasing thermodynamic stability of PDG.<sup>22</sup> This reduced stability is seen herein for TNB in the higher enthalpy for the PDG compared to the CG (Fig. 3). The origin of this effect remains to be fully understood but is related to

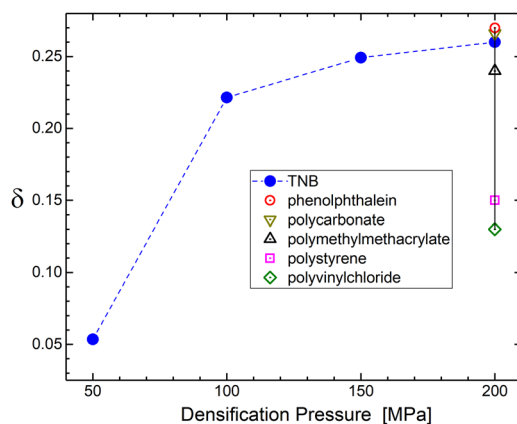


**FIG. 2.** Pressure densification parameter [Eq. (1)] for TNB at various pressures, along with literature results for various materials at  $P_1 = 200$  MPa.

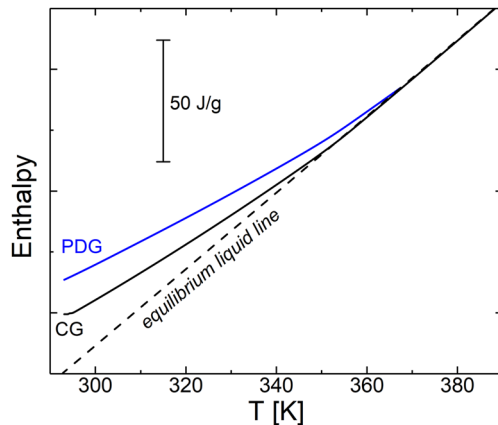


**FIG. 3.** Differential scanning calorimetry data ( $0.5 \text{ K min}^{-1}$ ) showing the lower stability of the pressure-densified TNB. The data shown are per mass, and although the PDG is denser, the curves are qualitatively unchanged if the enthalpy were expressed per unit volume. The dashed line is the linear extrapolation of the liquid data.

unstable structures formed at the higher vitrification temperature, inducing internal stresses, reduced free volume,<sup>44,45</sup> reduced local ordering,<sup>46</sup> and slightly more anharmonic vibrational motions.<sup>47</sup> Andersson and Johari<sup>27,28</sup> interpreted the reduced stability in terms of the lower entropy and higher thermal expansivity of PDG. However, Fig. 4 shows that for TNB, the temperature of the glass to liquid

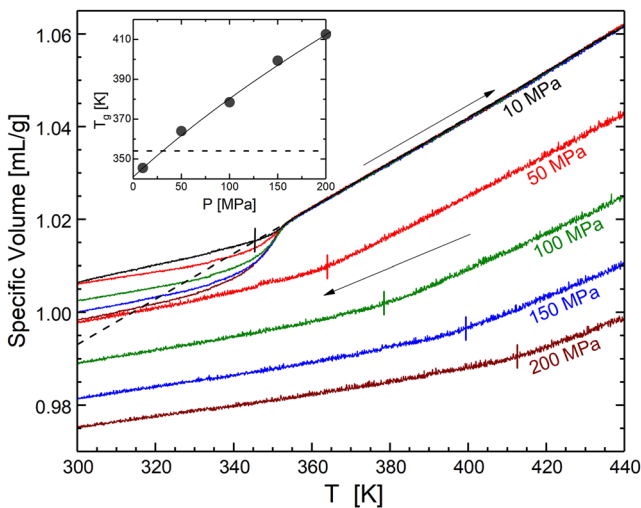


**FIG. 4.** Cooling of TNB at various pressures to 300 K (lower 4 curves), followed by heating after the pressure was reduced to 10 MPa (upper curves). Depending on  $P_1$  and the temperature, the density of PDG is above or below the extrapolated density (dashed line) of the equilibrium liquid. The inset shows the glass transition temperature for cooling at various pressures with the line at the fit of Eq. (2). These temperatures are indicated by short vertical lines in the main panel (the cooling curve for 10 MPa is not shown). The horizontal dashed line in the inset is the transition temperature ( $\approx 354 \text{ K}$ ) for heating at 10 MPa, which is independent of the vitrification pressure.

transition, indicated by the thermal expansivity assuming the value of the liquid, is independent of the vitrification pressure, despite the fact that the glass transition temperature measured for CG during cooling systematically increases with pressure (Fig. 4 inset). Fitting this  $T_g(P)$  data to the empirical Andersson equation,<sup>48</sup>

$$T_g(P) = T_g(0) \left( 1 + \frac{a}{b} P \right)^{1/a}, \quad (2)$$

with  $T_g(0) = 354 \text{ K}$ ,  $a = 3.15$ , and  $b = 769 \text{ MPa}^{-1}$ , the low pressure limiting value of the pressure coefficient of  $T_g$  for TNB is  $0.44 \text{ K/MPa}$ . This value is higher than literature values for other glass-forming materials.<sup>49</sup>

### Volume recovery and physical aging

In common with CG is slow structural equilibration of the PDG, accompanied by an increase in  $\rho$  toward its equilibrium value. The specific volume of the PDG is lower than that of the CG, but as can be seen in Fig. 4, it can be less or greater than the (extrapolated) equilibrium liquid volume, depending on temperature. To investigate the effect of proximity to the equilibrium density on physical aging, a PDG was formed at 200 MPa and after the release of the pressure, it was heated to various temperatures below  $T_g$ , followed by annealing at that temperature. The subsequent physical aging in all cases effected an increase in volume, independent of the equilibrium value (Fig. 5). For physical aging at temperatures not far from  $T_g$  ( $340 \leq T \text{ (K)} < 354$ ), the volume actually traverses the equilibrium volume to a higher value. This volume “overshoot” in aging of pressure densified glass has been observed previously.<sup>23–26</sup> For  $T < 315 \text{ K}$ , the specific volume of PDG is higher than the equilibrium value but, nevertheless, increases with aging time. The factor driving this aging process is the underlying glass structure, not the density.

This curious behavior of PDG was examined in detail for physical aging at  $T_g - 11 \text{ K}$  (Fig. 6). There is a relatively rapid change

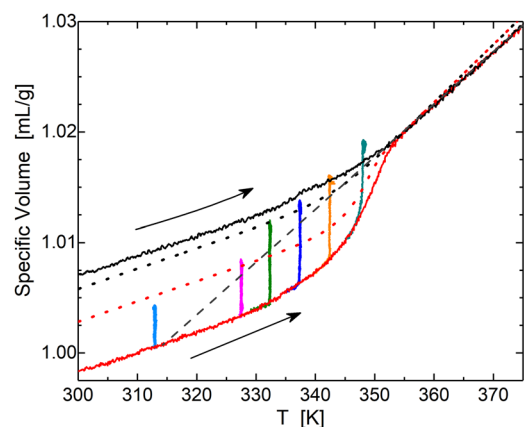


**FIG. 5.** The change in specific volume during physical aging of TNB ( $P_1 = 200 \text{ MPa}$ ) heated to different temperatures after release of the pressure, followed by aging at 10 MPa. The specific volume overshoots the equilibrium value (dashed line). The dotted lines are the predictions of the modified KAHR model [Eq. (6)].

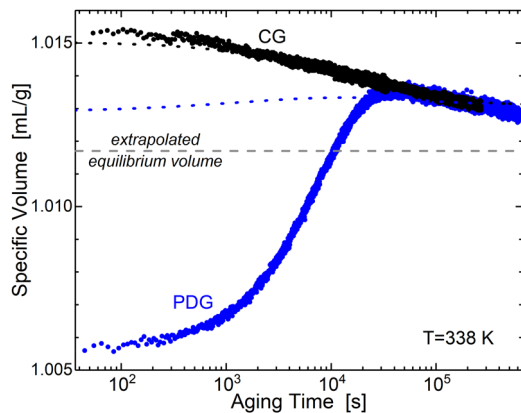


**FIG. 6.** Physical aging of TNB at  $T = T_g - 11$  K. Dotted lines show the prediction of the modified KAHR model for the two glasses [Eq. (6)].

in volume over the initial several hours, until the density of the CG is attained; we refer to this process as volume recovery. Upon further aging, the PDG and CG are indistinguishable. Evidently, the stressed regions in the PDG evolve initially to attain the structure of the CG, with subsequent slow aging toward equilibrium.<sup>27</sup> A similar response of the enthalpy has been reported during the aging of PDG.<sup>17,25,37,50</sup> The initial volume recovery of the PDG at various temperatures (Fig. 7) was fit to a stretched exponential function,

$$\frac{v(t) - v_i}{v_f - v_i} = 1 - \exp[-t/\tau_r]^\beta, \quad (3)$$

where  $v_i$  and  $v_f$  are the respective initial and final volumes,  $\beta$  is a constant, and  $\tau_r$  is the time constant for volume recovery. This strictly empirical equation has been shown to provide results comparable to those obtained using various models for aging of glasses.<sup>51</sup> Our best-fits are shown in the figure, with the recovery most “stretched” ( $\beta = 0.58$ ) at lower temperature (Fig. 7). The stretching exponent

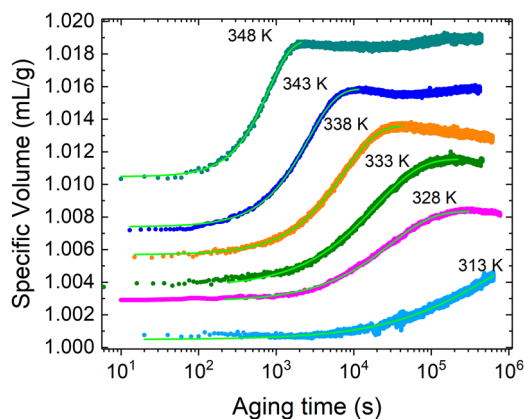


**FIG. 7.** Physical aging of TNB PDG at the indicated temperatures along with the fit of Eq. (3). Application of Eq. (6) (KAHR model) fails to describe the data, as seen in Fig. 6.

for the dielectric relaxation close to the glass transition is lower ( $\beta = 0.46$ ). If we make the assumption that the volume recovery involves the same reorientational motions that underlie the dielectric glass transition relaxation, the larger  $\beta$  for volume recovery suggests that the volume recovery accelerates as it proceeds and the volume increases. The  $\tau_r$  obtained by fitting Eq. (3) is then an effective relaxation time representative of the entire recovery process. The acceleration effect is stronger at higher aging temperatures, leading to larger  $\beta$ , but the reasons for this are unclear at this point.

Recovery times are plotted in Fig. 8 along with the reorientational relaxation times measured for TNB above  $T_g$ . The latter were obtained from dielectric measurements at 0.1 MPa and shifted to 10 MPa using a procedure based on the scaling property of the dynamics,<sup>52</sup> viz.,

$$\tau = f(T/\rho^\gamma), \quad (4)$$

where  $\gamma$  is a material constant and  $f$  is a function. The scaling exponent  $\gamma$  for TNB was determined using

$$\gamma = \frac{\partial \log T_g}{\partial \log \rho_g}, \quad (5)$$

in which  $\rho_g$  is the density at the glass transition; the glass temperatures and densities were taken from the PVT measurements. The result was  $\gamma = 6.0$  (see the inset of Fig. 8). Also plotted in this figure are the aging relaxation times  $\tau_{aging}$  obtained by fitting Eq. (3) to the volume of the CG, again fixing  $\beta$  to the value obtained dielectrically near  $T_g$  ( $\beta = 0.46$ ).

The relaxation times above  $T_g$  in Fig. 8 have the usual non-Arrhenius behavior. In the glassy state, changes in temperature have less effect on the density, so a change to a weaker  $T$ -dependence is expected. Previous work has shown that physical aging times for

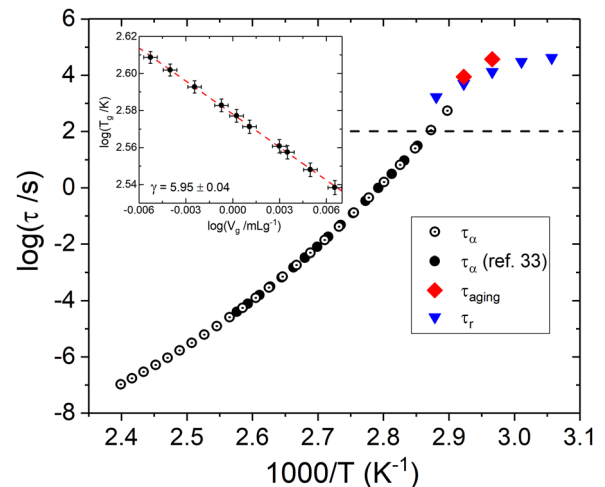


**FIG. 8.** Arrhenius plot of the dielectric relaxation times for TNB above  $T_g$  (defined by  $\tau_\alpha = 100$  s and indicated by the dashed horizontal line), along with the time constants for physical aging of the CG (diamonds). Also shown are recovery times for the PDG from Eq. (3). The inset is a double logarithmic plot of the density and temperature at the glass transition; the slope yields the indicated value of the scaling exponent [Eq. (5)].

glasses are comparable to the relaxation times of the corresponding liquid,<sup>53–55</sup> the latter obtained by extrapolation since they are too long to be measured below  $T_g$ . The data in Fig. 8 are not inconsistent with this idea, but inadequate to support it.

The recovery time for the PDG is as much as an order of magnitude shorter than the aging time at the two temperatures where both were measured. In that sense, unlike TNB glasses formed by vapor deposition, the PDG is less stable than the corresponding conventional glass at the same temperature, consistent with the former's higher enthalpy. However, the average recovery time at the highest temperature (very close to  $T_g$ ) is significantly longer than the equilibrium dielectric relaxation time  $\tau_\alpha$  at the same temperature.

There are several phenomenological models of the nonequilibrium behavior of glass-forming materials in response to changes in temperature; one of the most widely used of these, the Kovacs-Aklonis-Hutchinson-Ramos (KAHR) model,<sup>56</sup> has been extended by Ramos *et al.* to include the effects of pressure on the relaxation time.<sup>57</sup> For the evolution of the volume under an arbitrary temperature and pressure history, the model gives the expression

$$v = v_e + v_e \int_0^\xi \left[ -(\alpha_e - \alpha_g) \frac{dT}{d\xi'} - (k_e - k_g) \frac{dP}{d\xi'} \right] M(\xi - \xi') d\xi', \quad (6)$$

where  $\alpha$  is the thermal expansion coefficient,  $k$  is the isothermal compressibility, and the subscripts  $e$  and  $g$  refer to the equilibrium liquid and the glass, respectively. For the memory function  $M$ , we used a stretched exponential

$$M(\xi) = \exp \left[ - \left( \frac{\xi}{\tau_R} \right)^\beta \right], \quad (7)$$

in which  $\tau_R$  is the relaxation time at the reference state.  $\xi$  is the reduced time, defined as

$$\xi = \int_0^t \frac{\tau_R dt'}{\tau}, \quad (8)$$

and  $\tau$  is the material's relaxation time. The liquid equation of state determined using PVT measurements gives  $v_e$ ,  $\alpha_e$ , and  $k_e$ . Two additional equations of state were determined for the glass: one measured using isobaric cooling at various pressures (10–200 MPa) and the other from isothermal compression at various temperatures (303–363 K), both starting from the equilibrium liquid. From these, we obtained calculated  $\alpha_g$  and  $k_g$ . For the relaxation time, similar to Grassia *et al.*,<sup>58–60</sup> we used an expression derived from the Avramov model,<sup>52</sup>

$$\tau(T, V) = \tau_0 \exp \left[ \left( \frac{A}{TV^\gamma} \right)^\phi \right], \quad (9)$$

where  $\tau_0$ ,  $A$ , and  $\phi$  are material constants. Equation (9) satisfies the density scaling property [Eq. (4)] and describes equilibrium relaxation times accurately over a wide range of state points. Fitting (9) to the ambient pressure dielectric relaxation times using  $\gamma = 6.0$  as determined above, we obtain  $A = 949.5$ ,  $\phi = 2.84$ , and  $\log \tau_0 = -11.7$ . For simplicity, we take  $\beta = 0.46$ , which is the value determined for the dielectric relaxation peak near  $T_g$ . In this manner, the modified KAHR model [Eqs. (6) and (7)] has no adjustable parameters.

The dotted lines in Fig. 5 show the modified KAHR model's prediction, based on the actual pressure and temperature history used experimentally (for the volume during isobaric cooling of the CG and heating of the PDG). The modeled PDG is denser than the CG, but the pressure densification effect is much weaker than that observed experimentally, by about one-third. The prediction of the model for the evolution of the volume during aging of the CG and PDG is shown in Fig. 6. The model captures the aging behavior of the CG accurately. However, for the PDG, due to the underprediction of the degree of pressure densification, the initial volume is much higher than the experimental value. The modeled PDG volume does show a qualitatively correct behavior—a slight increase before it decreases to converge with that of the CG. Note that applying Eq. (9) for the relaxation time to the nonequilibrium state, as we do here, is not justified. Grassia and Simon<sup>61</sup> proposed a method that more accurately captures the out-of-equilibrium relaxation dynamics; however, the approach requires multiple adjustable parameters that cannot be determined herein from our experiments. By modifying the equation for the relaxation time, we can significantly change the location and shape of the  $v(T)$  curves around the glass transition, but this has a minimal effect on the amount of pressure densification predicted by the model. Another possible source of discrepancy is the fact that the modified KAHR model assumes the same kinetics for relaxation toward equilibrium after a volume change, regardless of whether it was caused by a change in temperature or pressure.<sup>57</sup> Further experimental work is required to examine the validity of this assumption.

## SUMMARY

TNB can be pressure densified to an extent that is among the largest observed for any organic material. By controlling the temperature, PDG was formed which had a density less than, equal to, or greater than the density of the corresponding CG. Unlike ultrastable TNB glass prepared using vapor deposition, pressure densified TNB exhibits higher enthalpy and lower thermal stability than the conventional glass formed at ambient pressure. TNB PDG exhibits anomalous physical aging, with the volume first increasing and reaching a maximum before finally decreasing toward the equilibrium volume. This behavior reflects two simultaneous processes: volume recovery, as the glass restructures following pressure densification, and the usual physical aging toward equilibrium. These two processes, associated with an increase and a decrease in volume, respectively, have different kinetics. In an analogous way to physical aging, the volume recovery can be described phenomenologically as having a time dependent relaxation time that changes (decreases) as the glass evolves from its pressure densified state toward a structure closer to the equilibrium one.

The role of pressure in the creation of metastable glasses has broad significance. For example, formation of the low and high density forms of amorphous water is affected by pressure, and bulk water under pressure forms a disordered solid rather than a crystal.<sup>62–64</sup> Thus, pressure densification experiments can provide insights into this complex and important liquid. To better understand the effects of vitrification under pressure, we are currently carrying out molecular dynamic simulations of TNB. Using the concept of fictive temperature and pressure to characterize the nonequilibrium state of the material, the objective is to gain a more

fundamental understanding of the structural changes accompanying recovery and aging of PDG.

## ACKNOWLEDGMENTS

This work was supported by the Office of Naval Research, in part by Code 332 (R. G. Barsoum). A.P.H. acknowledges an American Society for Engineering Education/Naval Research Laboratory postdoctoral fellowship.

## REFERENCES

- O. S. Narayanaswamy, "Stress and structural relaxation in tempering glass," *J. Am. Cer. Soc.* **61**, 146–152 (1978).
- Y. Qiu, Y. W. Bao, X. G. Liu, X. F. Wang, and D. T. Wan, "Effect of tempering process on the elasticity of soda-lime glass," *Rare Met. Mat. Eng.* **38**, 1133–1135 (2009).
- Z. Yin, F. Hannard, and F. Barthelat, "Impact-resistant nacre-like transparent materials," *Science* **364**, 1260–1263 (2019).
- B. Krour, F. Bernard, S. Benyoucef, and B. Fahsi, "Influence of the lamination on the redundancy of a horizontally layered glass element and analysis of the debonding of the adhesive interlayer," *Int. J. Adhes. Adhes.* **64**, 116–127 (2016).
- D. C. Ford, D. Hicks, C. Oses, C. Toher, and S. Curtarolo, "Metallic glasses for biodegradable implants," *Acta Mater.* **176**, 297–305 (2019).
- Y.-C. Hu, J. Schroers, M. D. Shattuck, and C. S. O'Hern, "Tuning the glass-forming ability of metallic glasses through energetic frustration," *Phys. Rev. Mater.* **3**, 085602 (2019).
- J. C. Qiao, Q. Wang, J. M. Pelletier, H. Kato, R. Casalini, D. Crespo, E. Pineda, Y. Yao, and Y. Yang, "Structural heterogeneities and mechanical behavior of amorphous alloys," *Prog. Mater. Sci.* **104**, 250–329 (2019).
- H. Osamu, S. Hiroshi, and S. Syúzô, "New finding of three kinds of glassy state for cyclohexene as a single compound," *Chem. Lett.* **2**, 79–82 (1973).
- M. D. Ediger, "Perspective: Highly stable vapor-deposited glasses," *J. Chem. Phys.* **147**, 210901 (2017).
- D. P. Erhard, D. Lovera, R. Giesa, V. Altstadt, and H. W. Schmidt, "Influence of physical aging on the performance of corona-charged amorphous polymer electrets," *J. Polym. Sci., Part B: Polym. Phys.* **48**, 990–997 (2010).
- G. P. Johari, "Electric field for increasing the solubility of glass - a much sought after pharmaceutical advantage," *J. Non-Cryst. Solids* **489**, 27–32 (2018).
- A. Gujral, L. Yu, and M. D. Ediger, "Anisotropic organic glasses," *Curr. Opin. Solid State Mater. Sci.* **22**, 49–57 (2018).
- J. M. Hutchinson, in *The Physics of Glassy Polymers*, edited by R. N. Haward (Springer, 1997), Chap. 3.
- R. Casalini and C. M. Roland, "Anomalous properties of the local dynamics in polymer glasses," *J. Chem. Phys.* **131**, 114501 (2009).
- H. W. Bree, J. Heijboer, L. C. E. Struik, and A. G. M. Tak, "The effect of densification on the mechanical properties of amorphous glassy polymers," *J. Polym. Sci.* **12**, 1857–1864 (1974).
- D. Fragiadakis and C. M. Roland, "A test for the existence of isomorphs in glass-forming materials," *J. Chem. Phys.* **147**, 084508 (2017).
- N. Rudolph, I. Kuhnert, E. Schmachtenberg, and G. W. Ehrenstein, "Pressure solidification of amorphous thermoplastics," *Polym. Eng. Sci.* **49**, 154–161 (2009).
- M. Guerette, M. R. Ackerson, J. Thomas, F. L. Yuan, E. B. Watson, D. Walker, and L. P. Huang, "Structure and properties of silica glass densified in cold compression and hot compression," *Sci. Rep.* **5**, 15343 (2015).
- J. B. Yourtee and S. L. Cooper, "Properties of densified amorphous polystyrene," *J. Appl. Polym. Sci.* **18**, 897–912 (1974).
- J. E. McKinney and R. Simha, "Thermodynamics of the densification process for polymer glasses," *J. Res. Natl. Bur. Stand., Sect. A* **81A**, 283–297 (1977).
- I. G. Brown, R. E. Wetton, M. J. Richardson, and N. G. Savill, "Glass transition and thermodynamic state of densified polymeric glasses," *Polymer* **19**, 659–663 (1978).
- A. P. Holt, D. Fragiadakis, J. A. Wollmershauser, B. N. Feigelson, M. Tyagi, and C. M. Roland, "Stability limits of pressure densified polycarbonate glass," *Macromolecules* **52**, 4139–4144 (2019).
- G. J. Kogowski and F. E. Filisko, "Experimental study of the density recovery of pressure-densified polystyrene glasses," *Macromolecules* **19**, 828–833 (1986).
- R. J. Roe and H. H. Song, "Isothermal relaxation of volume and density fluctuation of polystyrene glass prepared under elevated pressure," *Macromolecules* **18**, 1603–1609 (1985).
- A. Weitz and B. Wunderlich, "Thermal-analysis and dilatometry of glasses formed under elevated pressure," *J. Polym. Sci.* **12**, 2473–2491 (1974).
- S. Vleehouwers and E. Nies, "Selected thermodynamic aspects of the influence of pressure on polymer systems," *Thermochim. Acta* **238**, 371–395 (1994).
- O. Andersson and G. P. Johari, "Sub- $T_g$  features of glasses formed by cooling glycerol under pressure - Additional incompatibility of vibrational with configurational states in the depressurized, high density glass," *J. Chem. Phys.* **145**, 204506 (2016).
- G. P. Johari and O. Andersson, "Structural relaxation and thermal conductivity of high-pressure formed, high-density di-*n*-butyl phthalate glass and pressure induced departures from equilibrium state," *J. Chem. Phys.* **146**, 234505 (2017).
- D. J. Plazek, J. H. Magill, I. Echeverría, and I.-C. Chay, "Viscoelastic behavior of 1,3,5 tri- $\alpha$ -naphthyl benzene (will the real TaNB please stand up)," *J. Chem. Phys.* **110**, 10445–10451 (1999).
- S. F. Swallen, K. Traynor, R. J. McMahan, M. D. Ediger, and T. E. Mates, "Self-diffusion of supercooled tris-naphthylbenzene," *J. Phys. Chem. B* **113**, 4600–4608 (2009).
- R.-J. Ma, T.-J. He, and C. H. Wang, "A dynamic light scattering study of 1,3,5-tri- $\alpha$ -naphthyl benzene: A supercooled liquid," *J. Chem. Phys.* **88**, 1497–1500 (1988).
- R. K. Mishra and K. S. Dubey, "Analysis of thermodynamic parameters of glass forming polymeric melts journal of thermal analysis and calorimetry," *J. Therm. Anal. Calorim.* **62**, 687–702 (2000).
- K. Dawson, L. A. Kopff, L. Zhu, R. J. McMahan, L. Yu, R. Richert, and M. D. Ediger, "Molecular packing in highly stable glasses of vapor-deposited tris-naphthylbenzene isomers," *J. Chem. Phys.* **136**, 094505 (2012).
- K. Ishii and H. Nakayama, "Structural relaxation of vapor-deposited molecular glasses and supercooled liquids," *Phys. Chem. Chem. Phys.* **16**, 12073–12092 (2014).
- F. H. Stillinger, P. G. Debenedetti, and T. M. Truskett, "The Kauzmann paradox revisited," *J. Phys. Chem. B* **105**, 11809–11816 (2001).
- M. S. Beasley, C. Bishop, B. J. Kasting, and M. D. Ediger, "Vapor-deposited ethylbenzene glasses approach 'ideal glass' density," *J. Phys. Chem. Lett.* **10**, 4069–4075 (2019).
- G. P. Johari, "Comment on 'Water's second glass transition, K. Amann-Winkel, C. Gainaru, P. H. Handle, M. Seidl, H. Nelson, R. Böhmer, and T. Loerting, Proc. Natl. Acad. Sci. (U.S.) **110** (2013) 17720.', and the sub- $T_g$  features of pressure-densified glasses," *Thermochim. Acta* **617**, 208–218 (2015).
- P. Zoller, P. Bolli, V. Pahud, and H. Ackermann, "Apparatus for measuring pressure-volume-temperature relationships of polymers to 350 °C and 2200 kg/cm<sup>2</sup>," *Rev. Sci. Instr.* **47**, 948–952 (1976).
- D. Fragiadakis and C. M. Roland, "Chain flexibility and the segmental dynamics of polymers," *J. Phys. Chem. B* **123**, 5930–5934 (2019).
- N. I. Shishkin, "The vitrification of liquids and polymers under pressure: Part 5. The formation of condensed glasses," *Fiz. Tverd. Tela (Leningrad)* **2**, 350–357 (1960) [*Sov. Phys. (Sol. State)* **2**, 322–328 (1960) (in English)].
- M. Schmidt and F. H. J. Maurer, "Isotropic pressure-densified atactic poly(methyl methacrylate) glasses: Free-volume properties from equation of state data and positron annihilation lifetime spectroscopy," *Macromolecules* **33**, 3879–3891 (2000).
- R. E. Wetton and H. G. Money Penny, "Fundamental properties of densified polymer glasses," *Br. Polym. J.* **7**, 51 (1975).
- J. Curro and R.-J. Roe, "Small-angle x-ray scattering study of density fluctuation in pressure-densified polystyrene glasses," *J. Polym. Sci.* **21**, 1785–1796 (1983).

- <sup>44</sup>P. Destruel, B. Ai, and Hoang-The-Giam, "Dielectric results of polymeric glasses formed under hydrostatic pressure: Is the densified sample closer to thermodynamic equilibrium?," *J. Appl. Phys.* **55**, 2726–2732 (1984).
- <sup>45</sup>M. Schmidt, M. Olsson, and F. H. J. Maurer, "Macroscopic pressure–volume–temperature properties versus free-volume characteristics of isotropic pressure-densified amorphous polymer glasses," *J. Chem. Phys.* **112**, 11095–11106 (2000).
- <sup>46</sup>H.-H. Song and R. J. Roe, "Structural change accompanying volume change in amorphous polystyrene as studied by small and intermediate angle x-ray scattering," *Macromolecules* **20**, 2723–2732 (1987).
- <sup>47</sup>M. Schmidt, A. Brodin, P. Jacobsson, and F. H. J. Maurer, "Quasi-elastic Raman scattering and free volume in isotropic pressure-densified atactic poly(methyl methacrylate) glasses," *J. Chem. Phys.* **112**, 1020–1028 (2000).
- <sup>48</sup>S. P. Andersson and O. Andersson, "Relaxation studies of poly(propylene glycol) under high pressure," *Macromolecules* **31**, 2999–3006 (1998).
- <sup>49</sup>C. M. Roland, S. Hensel-Bielowka, M. Paluch, and R. Casalini, "Supercooled dynamics of glass-forming liquids and polymers under hydrostatic pressure," *Rep. Prog. Phys.* **68**, 1405–1478 (2005).
- <sup>50</sup>W. M. Prest and F. J. Roberts, "Enthalpy recovery in pressure-vitrified and mechanically stressed polymeric glasses," *Ann. N. Y. Acad. Sci.* **371**, 67–86 (1981).
- <sup>51</sup>R. Richert, P. Lunkenheimer, S. Kastner, and A. Loidl, "On the derivation of equilibrium relaxation times from aging experiments," *J. Phys. Chem. B* **117**, 12689–12694 (2013).
- <sup>52</sup>R. Casalini, U. Mohanty, and C. M. Roland, "Thermodynamic interpretation of the scaling of the dynamics of supercooled liquids," *J. Chem. Phys.* **125**, 014505 (2006).
- <sup>53</sup>Z. Wojnarowska, C. M. Roland, K. Kolodziejczyk, A. Swiety-Pospiech, K. Grzybowska, and M. Paluch, "Quantifying the structural dynamics of pharmaceuticals in the glassy state," *J. Phys. Chem. Lett.* **3**, 1238–1241 (2012).
- <sup>54</sup>R. Casalini and C. M. Roland, "Aging of a low molecular weight poly(methyl methacrylate)," *J. Non-Cryst. Solids* **357**, 282–285 (2011).
- <sup>55</sup>R. Casalini and C. M. Roland, "Aging of the secondary relaxation to probe structural relaxation in the glassy state," *Phys. Rev. Lett.* **102**, 035701 (2009).
- <sup>56</sup>A. J. Kovacs, J. J. Aklonis, J. M. Hutchinson, and A. R. Ramos, "Isobaric volume and enthalpy recovery of glasses. II. A transparent multiparameter theory," *J. Polym. Sci.* **17**, 1097–1162 (1979).
- <sup>57</sup>A. R. Ramos, A. J. Kovacs, J. M. O'Reilly, J. J. Tribone, and J. Greener, "Effect of combined pressure and temperature changes on structural recovery of glass-forming materials. I. Extension of the KAHR model," *J. Polym. Sci., Part B: Polym. Phys.* **26**, 501–513 (1988).
- <sup>58</sup>L. Grassia, M. G. Pastore Carbone, G. Mensitieri, and A. D'Amore, "Modeling of density evolution of PLA under ultra-high pressure/temperature histories," *Polymer* **52**, 4011–4020 (2011).
- <sup>59</sup>L. Grassia and A. D'Amore, "Isobaric and isothermal glass transition of PMMA: pressure-volume-temperature experiments and modelling predictions," *J. Non-Cryst. Solids* **357**, 414–418 (2011).
- <sup>60</sup>L. Grassia, M. G. Pastore Carbone, and A. D'Amore, "Modeling of the isobaric and isothermal glass transitions of polystyrene," *J. Appl. Polym. Sci.* **122**, 3752–3757 (2011).
- <sup>61</sup>L. Grassia and S. Simon, "Modeling volume relaxation of amorphous polymers: Modification of the equation for the relaxation time in the KAHR model," *Polymer* **53**, 3613–3620 (2012).
- <sup>62</sup>M. M. Koza, T. Hansen, R. P. May, and H. Schober, "Link between the diversity, heterogeneity and kinetic properties of amorphous ice structures," *J. Non-Cryst. Solids* **352**, 4988–4993 (2006).
- <sup>63</sup>O. Andersson, "Glass–liquid transition of water at high pressure," *Proc. Natl. Acad. Sci. U. S. A.* **108**, 11013–11016 (2011).
- <sup>64</sup>J. S. Tse and D. D. Klug, "Pressure amorphized ices – an atomistic perspective," *Phys. Chem. Chem. Phys.* **14**, 8255–8263 (2012).